# Inductive Fault Analysis of a Microresonator

Tao Jiang, Chris Kellon and R.D. (Shawn) Blanton
Electrical and Computer Engineering Department
Carnegie Mellon University
Pittsburgh, PA 15213 USA

## ABSTRACT

We study the failure mechanisms of a microresonator. A MEMs process simulation tool is used to discover the full spectrum of defective structures caused by particulate contaminations introduced during manufacturing. Based on process simulation results, defect categorization is performed. Mechanical and electrical simulation are then used to quantify the misbehaviors associated with the categories of defective structures. The analysis reveals that particulates can cause both parametric and catastrophic changes in behavior. Also, we found types of defects that do not affect mechanical behavior but have a significant impact on electrical behavior.

***Keywords***: microresonator, particulate contaminations, defect classification, MEMS test

## I. INTRODUCTION

High-volume production of MEMS-based systems will require cost-effective testing techniques to screen defective devices from good ones. Most current industrial practice rely on characterization tests and design validation tests for detecting defects. This may be problematic since:

1. characterization/validation tests target only portions of the functionality and hence may miss specific failure modes,
2. are applicable only for a specific design and,
3. may be inefficient in that simpler, less expensive tests may be sufficient.

In our work, we are attempting to develop generic fault models for capacitive inertial sensors and actuators that are fabricated using surface-micromachined technologies [1-3]. Generic fault models are desirable because of their applicability to a wide range of devices. Accurate fault models also enable pre-manufacture evaluation, thus allowing for test method optimization. Some effort has been placed in transferring mixed-signal test techniques to MEMS. In [4-6], an electrical schematic is used to model both the mechanical and electrical components of MEMS. Faults are modeled by adding or removing components from the schematic representation. Unfortunately, knowledge of failure modes is not used to determine the components that should be added or removed from the schematic. In [7], the failure mechanisms of a CMOS-compatible MEMS process were classified based on their impact on key transducer parameters. Our past work used process simulation and FEA[8] to understand the mechanical misbehaviors due to particulate contaminations. Here, we completely categorize our work in [9], and also extend the results to the electrical domain.

The rest of this paper is organized as follows. Section 2 gives an overview of our simulation environment. Section 3 provides details of the process simulation environment and enumerates the categories of defective structures resulting from particulate contaminations. Sections 4 and 5 describe the mechanical and electrical simulation components along with examples of mechanical and electrical misbehaviors. Finally, in Section 6 we summarize our contribution.

## II. SIMULATION ENVIRONMENT

For our analysis, we use the surface-micromachined microresonator[1] because it possesses all of the basic structures, such as the shuttle mass, spring beam, comb-finger, and anchor, which form the core primitives of a MEMS design library [10]. Many useful MEMS devices, such as accelerometers and gyroscopes, are formed by interconnecting these primitives. Thus, the analysis of the failure modes of the simple resonator structure will be applicable to other, more complex MEMS.

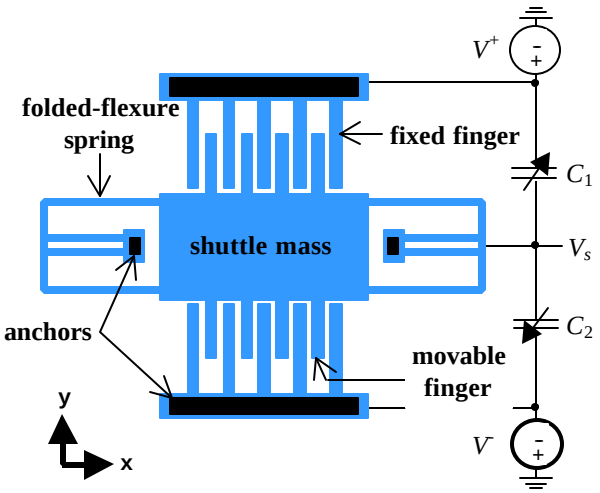


**Figure 1.** Resonator structure and the corresponding sensing capacitance circuit formed from the resonator.

[1] For the purpose of clarity, we will refer to the microresonator as simply as the "resonator".

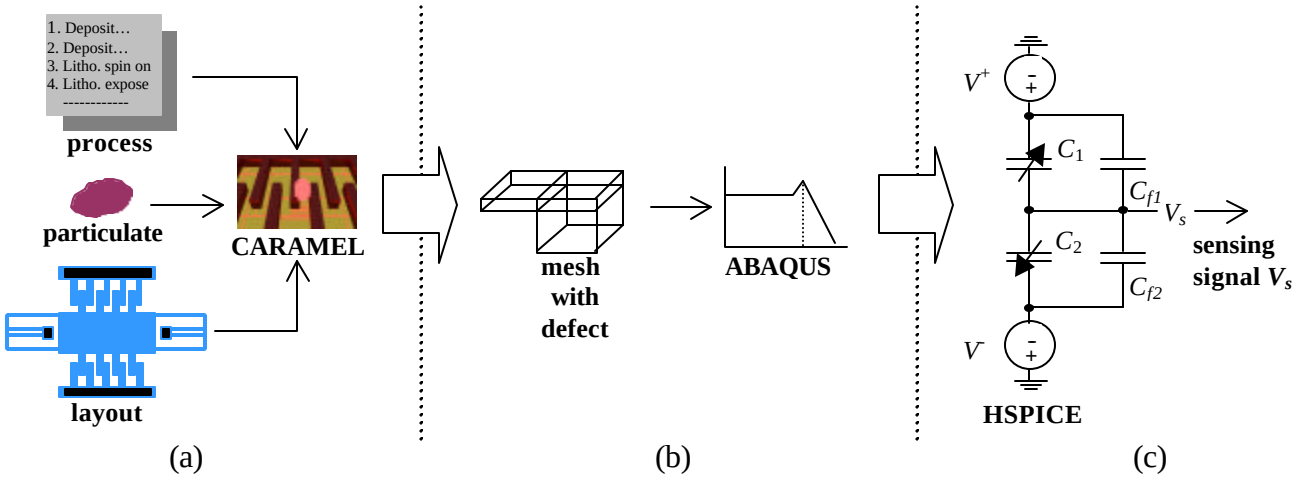


**Figure 2.** Simulation environment for the development of generic fault models for MEMS: (a) The tool CARAMEL [9] accepts a process description, particulate information, and a layout; it generates a mesh that captures the impact of the defect on the microstructure. (b) Mechanical simulation is performed using the FEA tool ABAQUS to determine the effect of the resulting defect on the mechanical properties of the microstructure. (c) Finally, HSPICE is used to determine the impact of the particulate on the electrical characteristics of the microstructure.

Figure 1 shows the structure of a resonator with all the primitive elements identified. The resonator is suspended above the substrate and is attached only at the four anchor locations shown. The shuttle mass is a block of material (typically polysilicon) which is suspended above the substrate by folded-flexure spring beams on either side. The spring is designed to be compliant in the *y* direction, but stiff in the *x* direction. This design characteristic is used to ensure that the resonator is most sensitive to only one direction of movement. Attached to the remaining two sides of the shuttle are sets of equally spaced beams called fingers. Opposite the shuttle fingers are the fixed fingers, so-called because they are securely anchored to the substrate. The inter-digited forms a set of parallel-plate, differential capacitors that transduces shuttle displacement into a capacitance change. Specifically, when an acceleration in the *y* direction is applied to the microstructure, the shuttle mass will move in the opposite direction due to an inertial force but will also experience a restoring force from the spring. At equilibrium, the shuttle mass will have a displacement from its original position. The displacement of the shuttle mass is proportional to the voltage signal $V_s$, a capacitive voltage generated by the two parallel-plate capacitors.

Figure 2 shows the stages of our simulation environment. The first stage is process simulation; it is used to generate the full spectrum of defective structures induced by particulate contaminants. The next two stages, mechanical and electrical simulation, are used to evaluate the misbehaviors of the defective structures revealed in the process simulation stage. Mechanical simulation can determine the displacement of the shuttle mass under an applied inertial force, while electrical simulation can determine the pertinent characteristics of the output sensing voltage $V_s$.

## III. STRUCTURAL DEFECTS

In this study, we assume MUMPs (Multi-Users MEMs Processes[1]) is used to manufacture the resonator. Four thousand process simulations were conducted using CARAMEL [9]. These particles were distributed randomly across all process steps and throughout the bounding-box area of the device. The size distribution of the particles ranged from 2µm to 4µm. Most particles missed the active area of the structure or were removed along with temporary layers during the processing. A total of 492 defective structures were finally generated.

Based on the resulting geometrical properties, defects are classified into three categories: surface, anchor and broken structure.

**Surface defects.** Surface defects are caused by particles introduced onto the surface of the suspended structure. There are several subtypes associated with this category.

- Surface non-finger protrusion defects are caused by particles adhering to the surface of the structural layer. The only impact of these defects is a small increase in resonator mass. This defect is always caused by particles introduced after the removal of the structural layer photoresist or the final release. (See Fig. 3a.)
- Surface finger protrusion defects are caused by particles located on the surface of two adjacent comb fingers, introduced after the removal of the structural layer photoresist or during the final release. These defects weld the two fingers together. (See Fig. 3b.)
- Lateral finger protrusion defects reduce the gap between comb fingers. They are caused by particles occurring after the photoresist deposition step for the

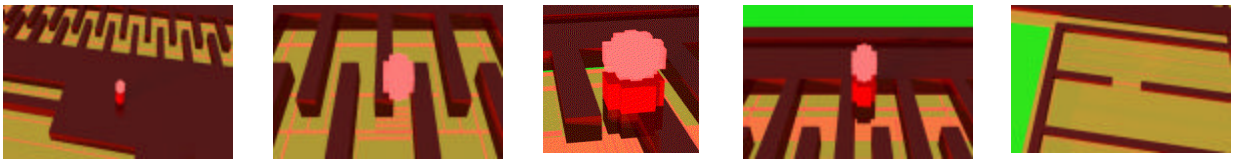

(a) (b) (c) (d) (e)

**Figure 3.** Representative examples of the defect categories caused by particles: (a) Surface protrusion located on the shuttle (b) surface finger protrusion that welds two adjacent fingers, (c) lateral finger protrusion that reduces finger gap in the overlap region, (d) surface finger protrusion that lies outside the overlap region of two adjacent fingers, and (e) broken spring beam.

structural layer. This defect type can be further sub-divided, based on the location and amount of gap reduction:

1. *Overlap, sticking:* protrusion is located in the overlap region of two fingers, and is large enough to weld the fingers together.

2. *Overlap, non-sticking:* protrusion is located in the overlap region of two fingers but is large enough to only reduce the gap. (See Fig. 3c.)

3. *Non-overlap, sticking:* protrusion is outside the overlap region of two fingers but may cause sticking during shuttle movement. (See Fig. 3d.)

4. *Non-overlap, non-sticking:* protrusion is outside the overlap region of two adjacent fingers but may reduce gap during shuttle movement.

**Anchor defects.** Anchor defects are caused by particles located between the substrate and suspended structure. They impede resonator movement under an applied inertial force. Anchor defects come from particles occurring before the structural layer deposition. There are two subtypes associated with this category of defects.

- Mass and finger defects cause an anchor under the shuttle mass or comb-fingers.

- Spring beam defects cause an anchor under a spring beam.

**Broken structure defects.** Broken structure defects are caused by particles introduced before the photoresist deposition for the structural layer. Presence of the particle during this step creates a vulnerable location in the structural material at the location of the particle. The over-etching that takes place at this location creates a broken structure. There are three sub-defect types based on which element of the resonator is affected. Hence, there can be *broken shuttle*, *finger*, and *beam* defects. An example of a broken spring beam defect is shown in Figure 3e.

## IV. MECHANICAL MISBEHAVIORS

The defective structure generated by CARAMEL is represented as a mesh using three-dimensional cuboid elements. The generated mesh is completely compatible with the FEA tool ABAQUS [8]. FEA is used to determine the impact of defects on the mechanical frequency response of the resonator. It is used to study all categories of defective structures. Frequency response is analyzed because many key mechanical parameters, such as spring constant K, quality factor Q, and resonant frequency $f_0$, can be obtained from the spectrum. The displacement ***d*** of the resonator along the sensing axis *y* can also be determined from the spectrum. The displacement parameter ***d*** makes it possible to embed the resonator into an electric model of an accelerometer as a mechanical sensing component for electrical simulation.

The frequency spectrum curves were obtained by applying a sinusoidal acceleration signal with a magnitude of 100g in the *y* direction, and sweeping its frequency from 1Hz to 10 MHz. The spectrums obtained from our defect categories fall into four different classes:

Class 1: Spectrums in this class essentially match the defect-free case. Defects that include surface protrusions, lateral protrusions that do not cause sticking, and broken shuttles and fingers cause these spectrums since they either slightly increase or decrease the mass of the resonator.

Class 2: Spectrums in this class exhibit about an order of magnitude of reduction in displacement. Resonator movement has been seriously impeded (Figure 4) due to welded comb fingers or anchors under the shuttle mass or fingers.

Class 3: Spectrums in this class are caused by unwanted anchor defects along the spring beam. An additional spring beam anchor changes the spring constant; the amount of the change is obviously dependent upon its location. As the anchor location moves closer to the shuttle, the stiffer the spring beam becomes. In Figure 5, we show three representative cases of this family of spectrums.

Class 4: Spectrums in this class are the result of floppier spring beams caused by particles that break the spring beam. Figure 6 shows that resonators with a floppier spring have a displacement larger than the nominal case.

## V. ELECTRICAL MISBEHAVIORS

The mechanical analysis of the displacement value $d$ is used to create a model of the variable capacitors $C_1$ and $C_2$ for electrical simulation. Figure 2c is the differential sensing circuitry widely used in accelerometers [3]. $V^+$ and $V^-$ are high-frequency modulation signals that are $180^o$ out of phase. $C_{f1}$ and $C_{f2}$ are fixed-valued capacitors introduced to the electrical model to represent the additional sensing capacitance caused by lateral protrusion defects (see Figure 3c). The electrical model of Figure 2c is simulated using HSPICE to determine the impact of the various categories of defects on the output sensing signal $V_s$.

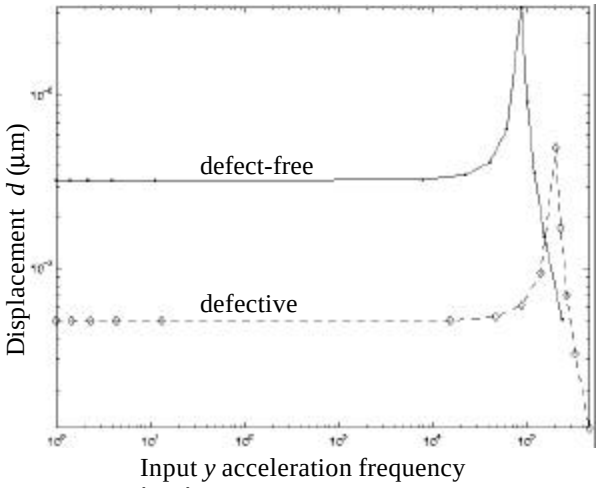


**Figure 4.** Comparison of defect-free frequency spectrum with the spectrum of a resonator affected by a welded fingers or anchors under the shuttle or fingers.

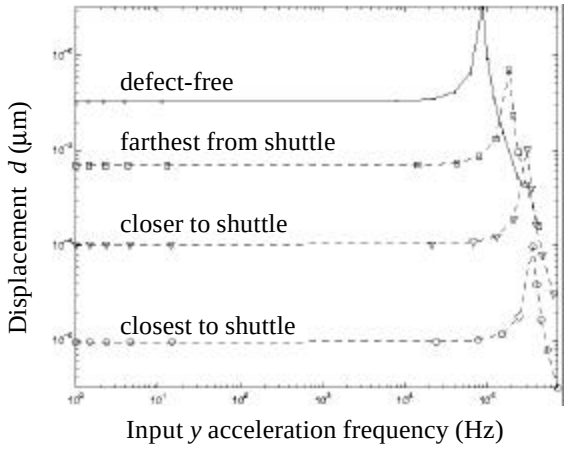


**Figure 5.** Representative spectrum curves of resonators affected by spring beam anchor defects.

For the defect–free situation, $V_s$ is proportional to the applied inertial force. For defective cases, $V_s$ will deviate from the nominal value anywhere from 5% to as much as 1000%. The importance of electrical simulation is that it can expose defects that only affect the sensing capacitance, such as a broken finger and a lateral finger protrusion that overlaps and is non-sticking. The misbehaviors associated with these defects are not revealed by FEA.

## VI. SUMMARY

We have classified all the possible defective structures exhibited by a microresonator structure affected by a single particulate contamination. The categorization is based on the mechanical and electrical misbehaviors associated with the various defects. Results show that particles can cause a wide range of changes in both the mechanical and electrical parameters of the resonator.

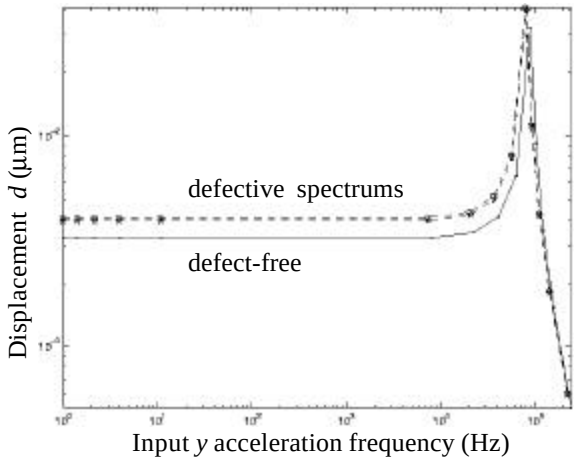


**Figure 6.** Comparison of a nominal frequency spectrum with the spectrums of resonators affected by a broken spring beam.

## REFERENCES


[1] D.A. Koester, et al. “Multi-user MEMS Processes (MUMPS) Introduction and Design Rules,” http://mems.mcnc.org/mumps.html, Oct. 1994.

[2] Sandia National Laboratories, “Intelligent MicroMachine Initiative," http://www.mdl.sandia.gov/Micromachine, P.O.Box 969, Livermore, CA 94551.

[3] Analog Devices Inc., "ADXL Series Accelerometer Datasheets," http://www.analog.com, One Technology Way, P.O. Box 9106, Norwood, MA 02062, 1996.

[4] T. Olbrich, A. Richardson, W. Vermeiren, B. Straube,, "Integrating Testability into Microsystems," *Microsystem Technologies*, pp. 72-79, Feb. 1997.

[5] W. Vermeiren, B. Straube, A. Holubek, "Defected-Oriented Experiments in Fault Modeling and Fault Simulation of Microsystem Components," *ED&TC*, pp. 522-527, Paris, March, 1996.

[6] M. Lubaszwski, E.F. Cota, and B. Courtois, "Microsystems Testing: an Approach and Open Problems," *DATE*, pp. 23-26, Paris, France, Feb. 1998.

[7] A. Castillejo, et.al. "Failure Mechanisms and Fault Classes for CMOS-Compatible Microelectromechanical Systems," *ITC*, Washington, USA, Oct. 1998.

[8] Hibbit, Karlsson & Sorensen Inc., “ABAQUS User Manual,” Vol. 2, Pawtucket, RI, 1995.

[9] A. Kolpekwar, C. Kellen and R.D. Blanton, "MEMS Fault Model Generation using CARAMEL," *ITC*, Washington, USA, Oct. 1998.

[10] J. E. Vandemeer, M. S. Kranz and G. K. Fedder, “Hierarchical Representation and Simulation of Micromachined Inertial Sensors,” *MSM*, Santa Clara, April, 1998.